Microcontact printing

White Electroluminescence from a Microcontact-Printing-Deposited CdSe/ZnS Colloidal Quantum-Dot Monolayer**

Aurora Rizzo,* Marco Mazzeo,* Mariano Biasiucci, Roberto Cingolani, and Giuseppe Gigli

The integration of colloidal semiconductor quantum dots (QDs) as lumophores into organic light-emitting-diode (LED) structures is becoming a promising field of scientific research.[1–10] Colloidal QDs are characterized by a high fluorescence efficiency, a narrow spectral emission and broadly tunable color-emission performance.[10–12] These properties, combined with the good photochemical stability of the covalently bonded colloidal nanocrystals,[13] are expected to increase the device lifetime at the high luminescence and current regimes necessary for lighting applications. Despite these potential advantages, there are still some limits to QD-LED fabrication, mainly due to the poor conduction properties of QD films compared to organic materials, determined by the organic capping layer that dresses the surface of the nanoparticles.[14] Consequently, in an electroluminescent hybrid device the exciton formation and the radiative recombination on colloidal QD sites is strongly inhibited.

In the past few years, several organic/inorganic hybrid device structures have been reported in the literature.[1–10] Amongst all the approaches, one of the most effective is to incorporate a QD monolayer between the electron and hole transport organic layers.[1–5] In this device structure colloidal nanocrystals act only as lumophores; they do not participate in the charge-conduction process. The organic layers transport charge carriers to the QD monolayer where recombination and radiative emission occur. Since colloidal nanocrystals cannot be evaporated, and can be deposited only by wet techniques,[1–8,15] two main strategies have so far been followed in order to get the monolayer onto the organic film.[1–5]

The first strategy, by Coe et al., exploits phase separation in a spin-coated host/guest blend of QDs and organic molecules,

[*] Dr. A. Rizzo, Dr. M. Mazzeo, M. Biasiucci, Prof. R. Cingolani, Prof. G. Gigli
NNL, National Nanotechnology Laboratory of CNR-INFM, Distretto Tecnologico ISUFI
Dipartimento di Ingegneria dell'Innovazione, Università del Salento
Via Arnesano Km 5, I-73100 Lecce (Italy)
Fax: (+39) 0832-29-82-30
E-mail: aurora.rizzo@unile.it; marco.mazzeo@unile.it
M. Biasiucci
Dipartimento di Fisica "E.R. Caianiello" Universita'
degli Studi di Salerno
via S. Allende, 84081 Baronissi SA (Italy)

namely N,N'-diphenyl-N,N'-bis(3-methylphenyl)-1,1'-biphenyl-4,4'-diamine (TPD).[1–3] During the spin-coating process the QDs tend to separate from the small molecules and form a single closely packed monolayer on the organic top surface. Monochromatic red- and green-emitting devices with a maximum external quantum efficiency of 2% have been obtained by using this approach.[1–3]

An alternative strategy for QD-LED fabrication was reported by Zhao et al.[4,5] Red-emitting CdSe/ZnS QDs were spin coated onto a thermally cross-linked hole-transporting layer, polystyrene (PS)-N,N'-diphenyl-N,N'-bis(4-n-butylphenyl)-1,1'-biphenyl-4,4'-diamine (TPD)–perfluorocyclobutane (PFCB). Following the deposition of the QD layer, the electron-transporting layer, 1,3,5-tris(N-phenylbenzimidazol-2yl) benzene (TPBI), was deposited by thermal evaporation. The maximum external quantum efficiency of these devices was 1.6% at 100 cd m^{-2}.[5]

Regarding hybrid white LEDs, few structure have been reported up to now.[6–8] To obtain white light, all three primary colors (red, green, and blue) have to be produced simultaneously. High-efficiency hybrid devices with emission originating only from the inorganic components have been fabricated using three CdSe/ZnS QDs of different sizes blended in an organic matrix, such as 4,4',N,N'-diphenylcarbazole (CBP)[7] or TPD.[8] However, all these device structures are seriously limited by the chemical properties of the materials employed and by the deposition technique. Using a wet technique, the independent processing of QDs and organic layers is not possible, resulting in a restriction in the choice of the hole-transporting material and in the number of organic under layers. This limits the potential for engineering the device structure and optimizing carrier injection and balance.

Microcontact printing (μCP) seems to be a promising technique to replace QD wet-deposition methods. In the standard μCP technique, a poly(dimethylsiloxane) (PDMS) stamp is inked by the material, which is then transferred onto the solid substrate by conformal contact of the elastomeric stamp and the substrate. However, this technique cannot be used for the deposition of colloidal semiconductor nanocrystals. In fact, the PDMS stamp is readily swelled by a number of nonpolar solvents, such as toluene and chloroform, in which nanocrystals for optoelectronic applications are usually dispersed. Consequently, conformal contact becomes very difficult, if not impossible. In order to prevent the swelling of the PDMS, Coe-Sullivan et al. modified the surface of the stamp by coating it with a chemical vapor deposited Parylene-C layer. However, using chemical vapor deposition makes the μCP technique more complicated and expensive.[9,16]

Herein we propose a new approach, based on μCP, using a SU-8 photoresist as a protective layer for the PDMS. We use this technique to fabricate a multilayer, hybrid, white-light-emitting diode. The advantage of using SU-8 instead of Parylene-C is the possibility for deposition by using a very easy and low-cost spin-coating process. Figure 1 displays a schematic sketch of the technique.

The PDMS mold was prepared by casting the poly (dimethylsiloxane) onto the top of a blank silicon master. After curing, the stamp was removed from the master and

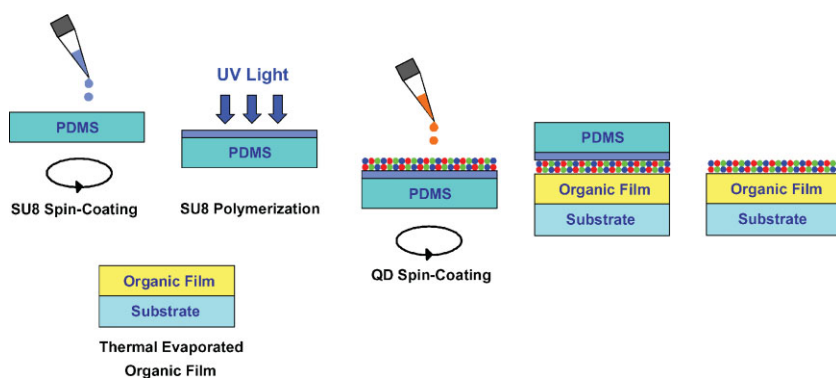WILEY InterScience®
DISCOVER SOMETHING GREAT

Figure 1. A schematic sketch of the modified µCP technique used to deposit colloidal nanocrystals on organic thin films.

SU-8 was spin-coated onto the top. The SU-8 was then exposed to UV radiation and subsequently thermally cross linked in order to make the film insoluble to toluene. A mixed blue, green, and red CdSe/ZnS- (respectively 59%, 17% and 24% by weight) QD solution was spin coated onto the SU-8 protected PDMS. The inked stamp was then inverted onto the surface of a previously evaporated organic thin film and peeled away after 30 seconds.

The quality of the transferred QD film was characterized by confocal microscopy. Figure 2 shows three images of the same QD area obtained by exciting the sample at 405 nm and collecting the emission in three different wavelength ranges: 465 nm–515 nm, in order to collect blue QD emission (Figure 2a), 525 nm–575 nm for the green QD emission

(Figure 2b), and 595 nm–655 nm for the red emission (Figure 2c). The corresponding photoluminescence (PL) spectra of the three CdSe/ZnS QDs are also shown (Figure 2d, e, and f). The resulting film is homogeneous and the three QD colors are uniformly deposited on the organic substrate.

Figure 3 shows atomic force microscopy (AFM) images of the same film. Figure 3a was taken at the interface between the CBP and QD layer at the edge of a pinhole defect. Using the profile (Figure 3b) we can estimate a QD film thickness of about 10 nm. In Figure 3c, d, e, and f AFM images of the QD film at different resolutions are shown. The images in Figure 3a, c, and d show the uniform distribution of the QDs on the organic material, with an average roughness of about 5 nm. Moreover, in the higher resolution images in Figure 3e and f it is possible to discriminate the two phases: QDs from 4–10 nm in diameter on the top and organic CBP as an under layer. In order to reduce the convolution tip effect these two images were acquired in noncontact mode by means of high-sensitivity ultra-sharp tip with radius less than 7 nm. However, a little broadening in size for the smaller QDs (diameter <7 nm) due to the tip effect was observed.

This as-prepared film was used for the fabrication of white-emitting hybrid LEDs. In Figure 4a we show a scheme of the fabricated multilayer device and the proposed energy-level
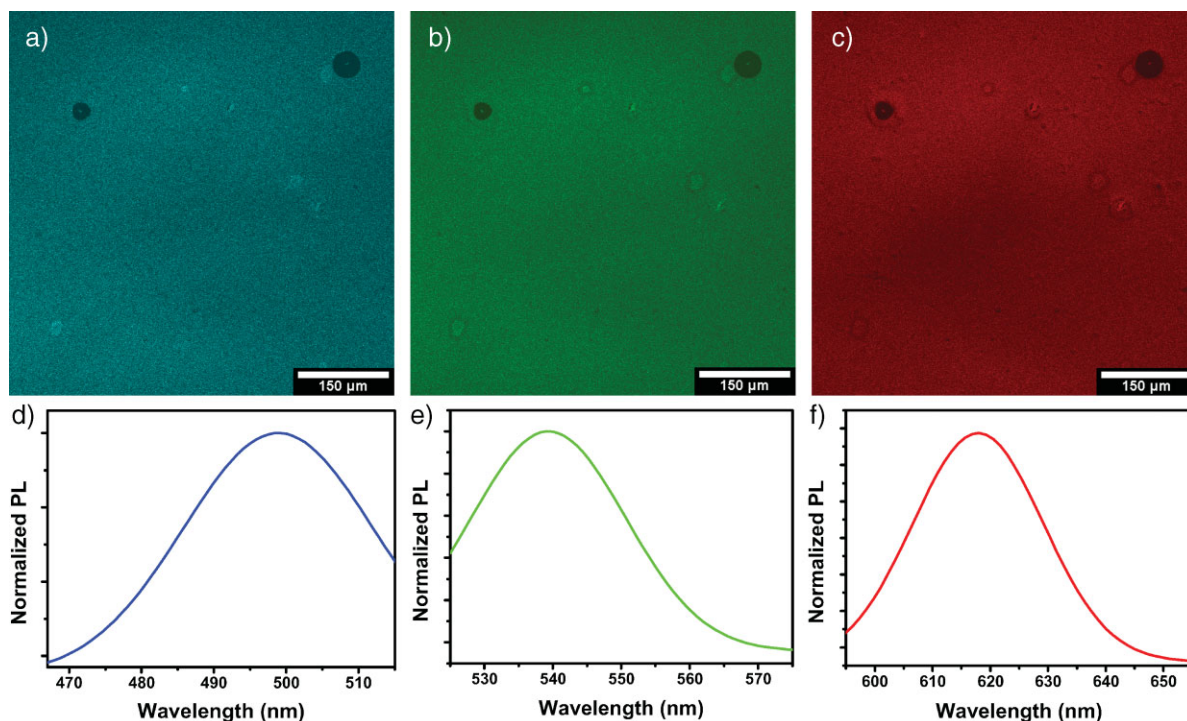

Figure 2. Confocal microscope characterization of the transferred nanocrystal layer. a)–c) Confocal images of the QD layer taken at different spectral windows: a) 465–515 nm, b) 525–575 nm, c) 595–655 nm. d)–f) Photoluminescence (PL) spectra of the same sample. Some pinhole defects are present in the film due to the spin coating process and the presence of aggregates in the QD solution.
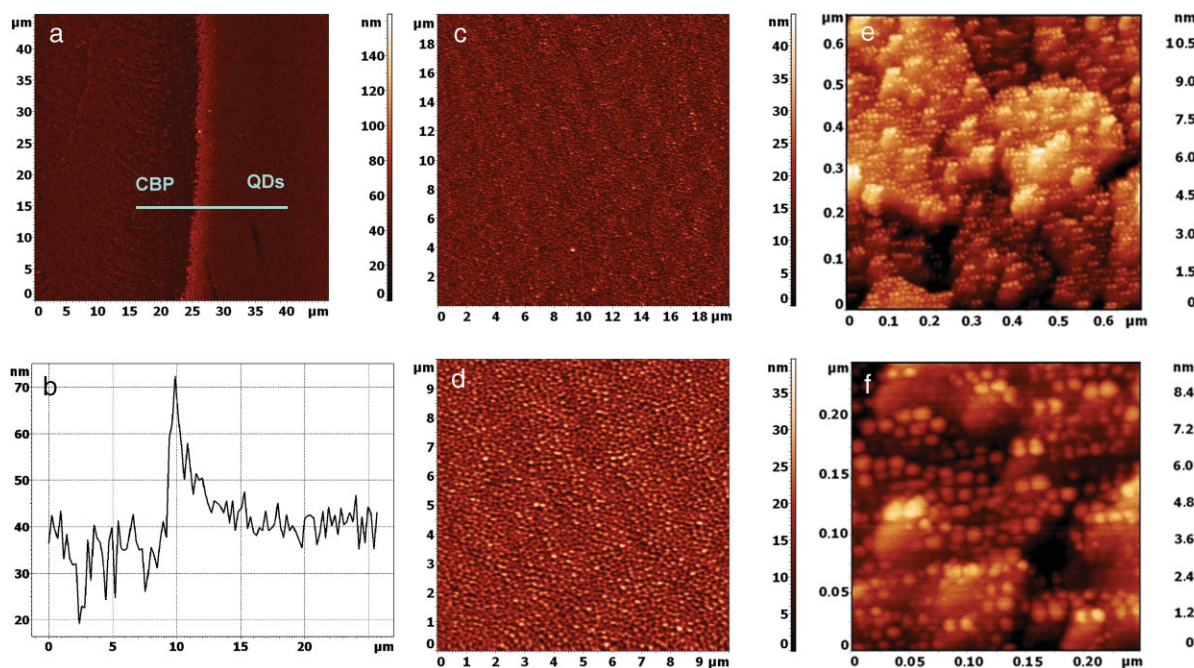
Figure 3. AFM characterization of the transferred nanocrystal layer. a) AFM image of the layer at the edge of a pinhole defect and b) the corresponding profile. c)–f) AFM images of the QD film with a scanning size of c) 20 μm, d) 10 μm, e) 650 nm, and f) 250 nm.

diagram.[17] For the CdSe/ZnS QDs the rough values for the electron affinity (EA) and ionization energy (IE) are shown for the red (−4.6 eV; −6.6 eV) and blue (−4.4 eV; −7.3 eV) samples.[1,6–8,10,18] Hole–injection and hole–transporting layers (HILs and HTLs, respectively) were thermally evaporated onto an indium tin oxide (ITO) substrate, then the QD layer was transferred onto the organic substrate by the μCP technique reported above. Hole-blocking and electron-transporting layers (HBLs and ETLs, respectively) were then finally evaporated on the QD film. LiF/Al was used as a cathode.

In order to improve the hole injection in the nanocrystal layer, a 40-nm HIL of N,N′-bis(naphthalen-1-yl)-N,N′-bis(phenyl)benzidine (α-NPD) doped with 2,3,5,6-tetra-fluoro-7,7,8,8-tetracyano-quinodimethane (F4-TCNQ) and a 30-nm HTL of CBP were used. F4-TCNQ molecules in the α-NPD matrix functioned as electron acceptors, removing electrons from the α-NPD highest occupied molecular orbital (HOMO) states in order to generate holes (p-type doping).[19] The 15-nm 2,9-dimethyl-4,7-diphenyl-1,10-phenanthroline (BCP) HBL's function was to block the transfer of both holes and excitons into the 20-nm ETL of tris(8-(hydroxyl-quinoline)) aluminum (Alq_3) and consequently to inhibit its emission.[1] The electroluminescence (EL) spectrum, the I-V characteristic, and the current efficiency (CE) of the device for different applied voltages are shown in Figure 4b and c. A maximum efficiency of about 0.4 cd A^{-1} was reached at 7 V and a current density of 10 mA cm^{-2}. Luminances of 150 cd m^{-2} at 10 V and 256 cd m^{-2} at 12 V were obtained. CIE coordinates were stable in the white region, varying from (0.40; 0.47) at 7 V to (0.37; 0.45) at 10 V.

Two dominant QD-excitation mechanisms were present in the hybrid device: Förster energy transfer and charge trapping.[7,8] The first is strongly dependent on the overlap of the absorption and PL spectra of the materials involved. In Figure 5, the absorption spectra of the organic materials and the emission/absorption spectra of red, green, and blue CdSe/ZnS QDs are shown. A clear overlap between the α-NPD, CBP, and Alq_3 emission and the absorption spectra of the three differently sized QDs allows for the possibility of a resonant energy transfer of excitons formed on organic sites to the QDs, according to Förster theory and experimental evidence.[6,7,20] Moreover, the spectral overlap between the emission and absorption of different nano-crystal sizes suggests that QD to QD Förster transfer is another possible pathway, in agreement with spectroscopic evidence of energy transfer in closed-packed CdSe-QD solids.[21]

In the charge-trapping process, electrons may be trapped in the QDs owing to the absence of any energy barrier between the organic Alq3 and BCP layers and CdSe/ZnS layer (see Figure 4a). For these charged QDs, the barrier to hole injection and transfer from the α-NPD/CBP bilayer is reduced. Thus, exciton formation and consequent radiative recombination occur on QD sites upon an acceptance of high-mobility holes from CBP.[1,7]

The electroluminescence spectra at different applied voltages appear in Figure 4b, showing an increase of the green and blue components relative to the red when the voltage is increased from 5 V to 10 V. This is consistent with the larger barrier for hole injection in the smaller QDs (see Figure 4a).[8] The presence of a α-NPD (420 nm) small-band emission is due to the presence of pinhole defects, grain boundaries, and interstitial spaces in the QD thin layer that allow the formation of excitons on organic sites. The HOMO level alignment of α-NPD/CBP suggests an accumulation of
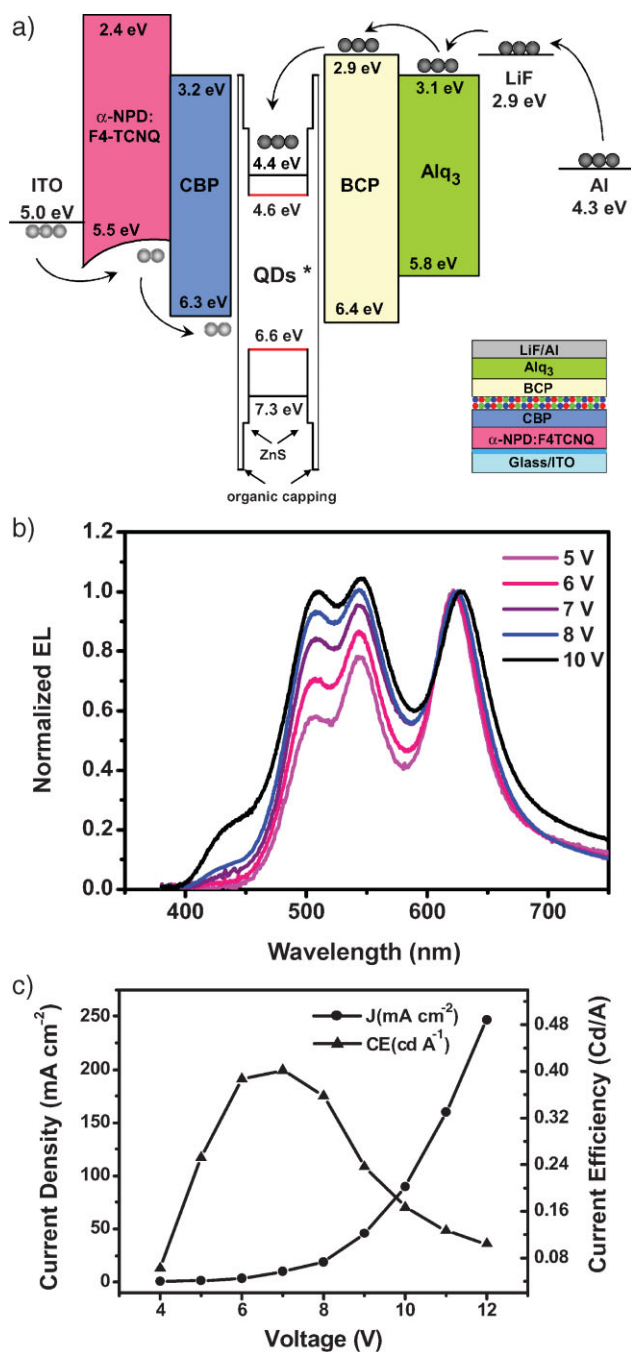
a)

b)

c)

Figure 4. Hybrid device characteristics. a) Proposed energy level diagram for the hybrid device and scheme of the device stack. b) EL spectra of the device at different applied voltages normalized at the red peak. c) I–V characteristic and current efficiency (CE) for the hybrid device.

Figure 5. Normalized PL for Alq_3 (green solid line), α-NPD (black solid line), CBP (blue solid line) and for the three sizes of CdSe/ZnS QD (blue, green and red solid lines); normalized absorption for the three sizes of QD (blue, green and red dash-dot lines).

of hybrid white multilayer-structure LEDs without any restrictions in the choice of organic material.

Experimental Section

QD deposition: The two-component silicon-based elastomer, PDMS Sylgard 184, was realized by making a mixture of pre-polymer and curing agent with a mixing ratio of 20:1. The PDMS mold was fabricated by casting the elastomer onto the top of a silicon master and curing at 65 °C for 1 h. SU-8 2010 from Microchem was spin-coated on the PDMS replica at 4000 rpm, pre-baked (1 min at 65 °C, 3 min at 95 °), UV polymerized for 5 min at 100 W and post-baked (1 min at 65 °C, 3 min at 95 °). A 30 nm layer of CBP was thermal evaporated at a pressure of 2.0×10^{-6} mbar onto ITO substrates. A mixed solution of red, green and blue core/shell CdSe/ZnS purchased from Evident Technologies was spin coated at 2000 rpm onto the PDMS pad protected by the SU-8 layer. The inked PDMS stamp was then brought into conformal contact with the CBP substrate for 30 s, and then peeled away. The morphology of the QD film was characterized by a confocal laser scanning microscope (FluoView1000, Olympus) using an excitation wavelength of 405 nm, by an AFM Solver Pro NT-MDT in a semicontact mode, and by an AFM XE-100 PSIA in noncontact mode.

Hybrid electroluminescent device: A 40 nm HIL and 30 nm HTL, respectively α-NPD doped with F4-TCNQ and CBP, were evaporated in sequence on cleaned ITO substrates. Then a mixed blue, green and red CdSe/ZnS QD layer was deposited on the organic materials by using the µCP technique. Finally, a 15-nm hole-blocking BCP layer and a 20-nm electron- transporting Alq_3 layer were deposited by thermal evaporation. All the organic materials

holes in the α-NPD at the HIL/HTL interface.[2] Increasing the voltage, and consequently the current, causes an increase in the fraction of emission coming from the organic layer.

In conclusion, we developed a dry, simple, and low-cost technique for deposition of colloidal semiconductor nanocrystals on organic-material layers. This technique allows the deposition of a homogeneous thin layer (about 10 nm) of mixed CdSe/ZnS red, green, and blue QDs. The independent processing of QD and organic material permits the fabrication
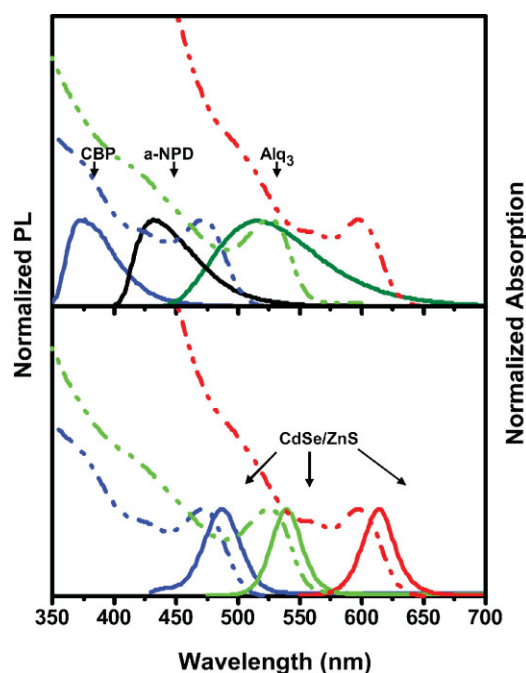
© 2008 Wiley-VCH Verlag GmbH & Co. KGaA, Weinheim

were thermal evaporated at a rate of 1Å s^{-1} at a pressure of 2×10^{-6} mbar. 0.5-nm lithium-fluoride (LiF) and 200-nm aluminum (Al) electrodes were evaporated through a contact shadow mask at a pressure of 4×10^{-6} mbar. EL spectrum and luminance were measured by using an OL 770 spectro-radiometer (Optronic Laboratories). The *I–V* characteristic was measured by using a Keithley 2400 source measurement unit. All the measurements were performed at room temperature in air without encapsulation.

[1] S. Coe, W. K. Woo, M. G. Bawendi, V. Bulović, *Nature* **2002**, *420*, 800.

[2] S. Coe-Sullivan, W. K. Woo, J. S. Steckel, M. G. Bawendi, V. Bulović, *Org. Electron.* **2003**, *4*, 123.

[3] S. Coe-Sullivan, J. S. Steckel, W. K. Woo, M. G. Bawendi, V. Bulović, *Adv. Func. Mater.* **2005**, *15*, 1117.

[4] J. Zhao, J. A. Bardecker, A. M. Munro, M. S. Liu, Y. H. Niu, I.-K. Ding, J. Luo, B. Chen, A. K.-Y. Jen, D. S. Ginger, *Nano Lett.* **2006**, *6*, 463.

[5] Y. H. Niu, A. M. Munro, Y.-J. Cheng, Y. Q. Tian, M. S. Liu, J. Zhao, J. A. Bardecker, I. J.-L. Plante, D. S. Ginger, A. K.-Y. Jen, *Adv. Mater.* **2007**, *19*, 3371.

[6] Y. Q. Li, A. Rizzo, M. Mazzeo, L. Carbone, L. Manna, R. Cingolani, G. Gigli, *J. Appl. Phys.* **2005**, *97*, 113501.

[7] Y. Q. Li, A. Rizzo, R. Cingolani, G. Gigli, *Adv. Mater.* **2006**, *18*, 2545.

[8] P. O. Anikeeva, J. E. Halpert, M. G. Bawendi, V. Bulović, *Nano Lett.* **2007**, *7*, 2196.

[9] J. S. Steckel, P. Snee, S. Coe-Sullivan, J. P. Zimmer, J. E. Halpert, P. Anikeeva, L. A. Kim, V. Bulović, M. G. Bawendi, *Angew. Chem. Int. Ed.* **2006**, *45*, 5796.

[10] A. Rizzo, Y. Q. Li, S. Kudera, F. Della Sala, M. Zanella, W. J. Parak, R. Cingolani, L. Manna, G. Gigli, *Appl. Phys. Lett.* **2007**, *90*, 051106.

[11] B. O. Dabbousi, J. Rodriguez-Viejo, F. V. Mikulec, J. R. Heine, H. Mattoussi, R. Ober, K. F. Jensen, M. G. Bawendi, *J. Phys. Chem. B* **1997**, *101*, 9463.

[12] a) P. Reiss, J. Bleuse, A. Pron, *Nano Lett.* **2002**, *2*, 781; b) S. Kudera, M. Zanella, C. Giannini, A. Rizzo, Y. Q. Li, G. Gigli, R. Cingolani, G. Ciccarella, W. Spahl, W. J. Parak, L. Manna, *Adv. Mater.* **2007**, *19*, 548.

[13] V. I. Klimov, *Los Alamos Sci.* **2003**, *28*, 214.

[14] a) C. A. Leatherdale, C. R. Kagan, N. Y. Morgan, S. A. Empedocles, M. A. Kastner, M. G. Bawendi, *Phys. Rev. B* **2000**, *62*, 2669; b) V. J. Porter, S. Geyer, J. E. Halpert, M. A. Kastner, M. G. Bawendi, *J. Phys. Chem.* **2008**, *112*, 2308.

[15] a) X. M. Lin, H. M. Jaeger, C. M. Sorensen, K. J. Klabunde, *J. Phys. Chem. B* **2001**, *105*, 3353; b) M. A. Islam, I. P. Herman, *Appl. Phys. Lett.* **2002**, *80*, 3823; c) V. Santhanam, J. Liu, R. Agarwal, R. P. Andres, *Langmuir* **2003**, *19*, 7881; d) V. Santhanam, R. P. Andres, *Nano Lett.* **2004**, *4*, 41.

[16] S. Coe-Sullivan, *PhD Thesis*, Department of Electrical Engineering and Computer Science, Massachusetts Institute of Technology, 2005.

[17] a) W. Y. Gao, A. Kahn, *J. Appl. Phys.* **2003**, *94*, 359; b) L. S. Hung, C. W. Tang, M. G. Mason, *Appl. Phys. Lett.* **1997**, *70*, 152; c) I. G. Hill, A. Kahn, *J. Appl. Phys.* **1998**, *84*, 5583; d) I. G. Hill, A. Kahn, *J. Appl. Phys.* **1999**, *86*, 4515.

[18] E. A. Weiss, R. C. Chiechi, S. M. Geyer, V. J. Porter, D. C. Bell, M. G. Bawendi, G. M. Whitesides, *J. Am. Chem. Soc.* **2008**, *130*, 74.

[19] K. Walzer, B. Maennig, M. Pfeiffer, K. Leo, *Chem. Rev.* **2007**, *107*, 1233.

[20] a) J. R. Lakowicz, *Principles of Fluorescence Spectroscopy*, Plenum Press, New York 1983; b) M. Anni, L. Manna, R. Cingolani, D. Valerini, A. Cretí, M. Lomascolo, *Appl. Phys. Lett.* **2004**, *85*, 4169.

[21] C. R. Kagan, C. B. Murray, M. G. Bawendi, *Phys. Rev. B* **1996**, *54*, 8633.